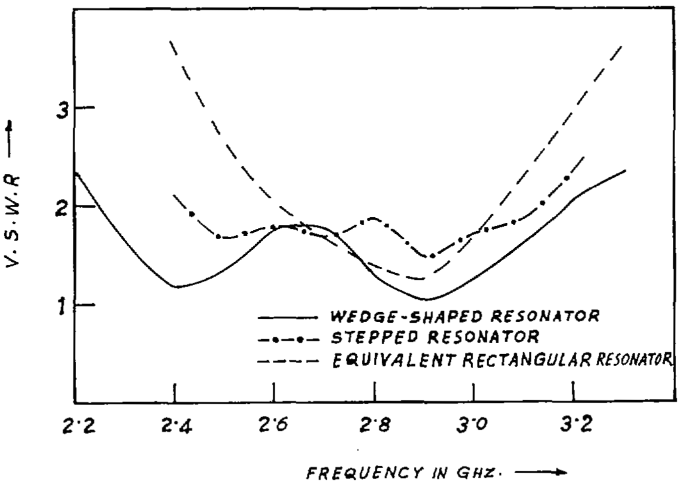

Fig. 2. VSWR versus frequency plot.

VSWR versus frequency plots of the resonators shown in Fig. 1 are given in Fig. 2. The (1:2) VSWR bandwidth of the microstrip resonator on a wedge-shaped dielectric is 28 percent and that on a stepped dielectric is 25 percent, whereas the bandwidth is 13 percent for an equivalent rectangular resonator. The maximum height for all the resonators was 0.01 m. This indicates that there is considerable improvement of bandwidth over that of a similar rectangular microstrip resonator. It may be mentioned that the feed point was in the same position for all the resonators.

ACKNOWLEDGMENT

The authors gratefully acknowledge the cooperation extended to them by Telecommunication Research Center, New Delhi and the Radar and Communication Center, I. I. T. Kharagpur for providing HP network analyzer measurement facility.

REFERENCES

[1] R. E. Munson, "Conformal microstrip antennas and microstrip phased arrays," *IEEE Trans. Antennas Propagat.*, vol. AP-22, no. 1, pp. 74–77, Jan. 1974.
[2] J. Q. Howell, "Microstrip antennas," *IEEE Trans. Antennas Propagat.*, vol. AP-23, pp. 90–93, Jan. 1975.
[3] J. Watkins, "Circular resonant structures in microstrip," *Electron. Lett.*, vol. 5, no. 21, pp. 524–525, Oct. 1969.
[4] A. G. Derneryd, "A theorectical investigation of the rectangular microstrip antenna," *IEEE Trans. Antennas Propagat.*, vol. AP-26, pp. 532–535, July 1978.
[5] Y. T. Lo *et al.*, "Theory and experiment on microstrip antennas," *IEEE Trans. Antennas Propagat*, vol. AP-27, no. 2, pp. 137–145, Mar. 1979.
[6] C. Wood, "Improved bandwidth of microstrip antennas using parasitic elements," *Proc. Inst. Elec. Eng. H, Microwaves, Opt. Acoust.*, vol. 127, pp. 231–234, Aug. 1980.
[7] A. G. Derneryd *et al.*, "Broad-band microstrip antenna element and array," *IEEE Trans. Antennas Propagat.*, vol. AP-29, no. 1, pp. 140–141, Jan. 1981.
[8] P. S. Hall *et al.*, "Wide bandwidth microstrip antennas for circuit integration," *Electron. Lett.*, vol. 15, no. 15, pp. 458–459, July 19, 1979.
[9] J. R. James *et al.*, "Design of microstrip antenna feeds, Part I: Estimation of radiation loss and design implications," *Proc. Inst. Elec. Eng. H, Microwaves, Opt. Acoust.*, vol. 128, Feb. 1981, pp. 19–25.

Cylindrical-Rectangular Microstrip Antenna

CLIFFORD M. KROWNE

Abstract—**Resonant frequencies f_r of a cylindrical-rectangular microstrip antenna are theoretically calculated. Comparison is made to f_r for a planar rectangular patch antenna, including the simplest planar patch modes having no field variation normal to the patch surface. The validity of using planar antenna patches to characterize microstrip antennas is examined.**

INTRODUCTION

In many applications pertaining to satellites, missiles, spacecraft, and aircraft, conformal microstrip antenna patches are used. Microstrip antenna patches are placed above what may be characterized as a conducting plane with a dielectric substrate separating the patch from the conducting plane [1]. However, often this plane surface is either distorted or the antenna elements are intentionally placed on a curved surface. Thus to determine the correct modal field solution to the electromagnetic cavity problem, which can be used to find the radiation field solution, this curvature should be taken into account. Here this is done for a rectangular patch on a cylindrical surface. The assumption that the conducting patch and the conducting cylinder (ground surface) act as electric walls, and that the open cavity ends act as magnetic walls is applied to the analysis for obtaining the fields and associated modal resonant frequencies [4]. This assumption should be particularly valid when using these fields for determining the radiation pattern for the limiting case of thin cavities ($h \ll a$) which are utilized for most microstrip antenna applications. All of the analysis for simplicity also assumes that the permittivity ϵ and permeability μ are constant (homogeneous medium filling cavity) and real (no dielectric losses).

The eigenvalue equations for resonant frequencies f_r are numerically solved and examined over a range of dielectric substrate thicknesses h. These resonant frequencies f_{rC} for the curved cylindrical-rectangular antenna, representing a distortion of a planar rectangular microstrip antenna, are compared to resonant frequencies f_{rR} of the planar patch antenna in order to assess the validity of the commonly used assumption that conformally mounted microstrip antennas may be treated as planar. The results demonstrate that this assumption is *good* for h that is small compared to the surface curvature a, and that it is *excellent* when considering excitation of the antenna with no spatial field variation normal to the surface.

THEORY

The geometry of the cavity is shown in Fig. 1 where Fig. 1(a) is a perspective drawing of a conducting patch on a cylindrical surface, Fig. 1(b) is a cross section through the patch and normal to the z-axis, and Fig. 1(c) shows the cavity isolated by itself in cross section. The conducting patch and grounded cylindrical surface are treated as electric walls and the magnetic walls of the cavity are defined by dropping perpendiculars from the patch

Manuscript received August 5, 1981; revised June 29, 1982.

The author is with the Electronics Technology Division, Naval Research Laboratory, Washington, DC 20375.

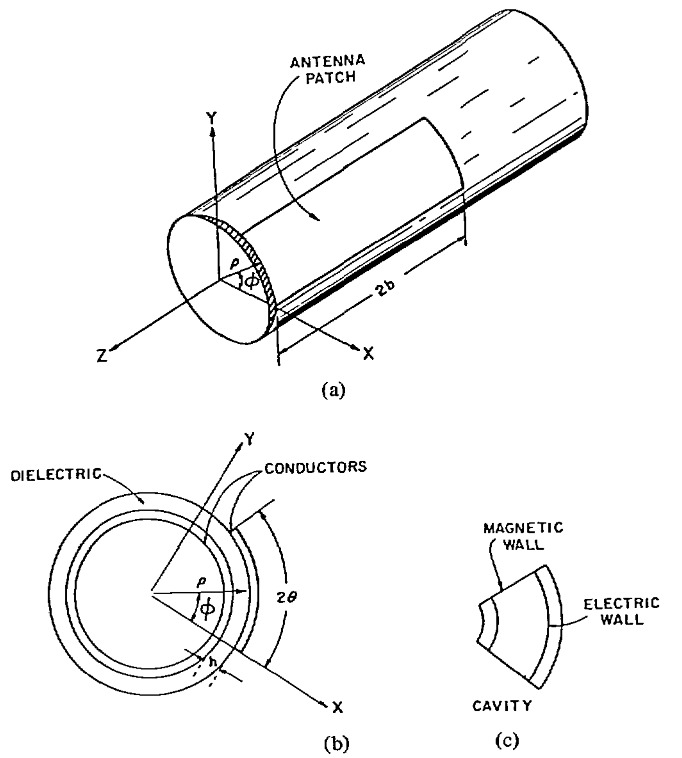

Fig. 1. (a) Perspective drawing of cylindrical-rectangular cavity. (b) Its cross section. (c) Cross section of cavity isolated to be by itself.

edges to the cylindrical conducting surface. The electric walls are located at $\rho = a$ and $\rho = a + h$ where h is the dielectric substrate thickness, and the magnetic walls are located at $z = 0, -2b$ and $\phi = 0, 2\theta$.

Below follows the derivation of the fields and eigenfrequencies for the transverse electric (TE_z) modes, transverse magnetic (TM_z) modes, and the limiting case modal results where the radial thickness h becomes vanishingly small.

The $\vec{E}$ and $\vec{H}$ phasor field solutions to Maxwell's harmonic equations in a source free cavity can be written as [3]

$$\vec{E} = -\nabla \times \vec{F} - j\omega\mu\vec{A} - \frac{j}{\omega\epsilon}\nabla(\nabla\cdot\vec{A}) \tag{1a}$$

$$\vec{H} = \nabla \times \vec{A} - j\omega\epsilon\vec{F} - \frac{j}{\omega\mu}\nabla(\nabla\cdot\vec{F}), \tag{1b}$$

where μ is the permeability and ϵ is the permittivity. $\vec{A}$ and $\vec{F}$ are arbitrary vector phasor potentials which satisfy the Helmholtz equations

$$\nabla^2\vec{F} + k^2\vec{F} = 0 \tag{2a}$$

$$\nabla^2\vec{A} + k^2\vec{A} = 0, \tag{2b}$$

where

$$k^2 = \omega^2\mu\epsilon. \tag{2c}$$

The TE to z field solution is constructed by choosing $\vec{A} = 0$ and $\vec{F} = \hat{u}_z\psi$ where $\hat{u}_z$ is the unit constant vector in the axial z-direction and ψ is a scalar function. The fields are known once ψ has been determined subject to the boundary conditions (BC) on $\vec{E}$ and $\vec{H}$ (Dirichlet conditions).

Using (1) and (2) and applying magnetic wall BC's, ψ can be expressed as

$$\psi_{mli} = A_{mli}R_v(k_{mi}\rho)\sin\left(\frac{m\pi}{2\theta}\phi\right)\cos\left(\frac{l\pi}{2b}z\right). \tag{3}$$

Here A_{mli} is a constant for the mlith mode, $m = 1, 2, \cdots$, and $l = 0, 1, \cdots$, $v = m\pi/2\theta$, and R_v satisfies Bessel's equation [4]-[6]

$$p\frac{d}{dp}\left[p\frac{dR_v(p)}{dp}\right] + [p^2 - v^2]R_v(p) = 0 \tag{4}$$

with $p = k_{mi}\rho$. Solutions to (4) are Bessel functions of the first kind J_v and of the second kind N_v which are linearly independent. Thus

$$R_v(p) = c_1J_v(p) + c_2N_v(p). \tag{5}$$

If the special case $\theta = \pi/2q$ occurs where q is an integer, then $v = mq$ is an integer, and J_v and N_v should be used to construct $R_v(p)$, otherwise J_{-v} may be used in place of N_v if $v \neq$ integer. Subjecting (5) to the electric wall BC's requires

$$R_v'(p)\,|_{\rho=a,\,a+h} = 0, \tag{6}$$

or

$$c_1J_v'(k_{mi}a) + c_2N_v'(k_{mi}a) = 0 \tag{7a}$$

$$c_1J_v'(k_{mi}[a+h]) + c_2N_v'(k_{mi}[a+h]) = 0 \tag{7b}$$

where the primes denote differentiation with respect to the argument. For there to be a nontrivial solution to (7), two linear equations in two unknowns c_1 and c_2, the determinant of the matrix formed by the c_i coefficients must be zero:

$$J_v'(k_{mi}a)N_v'(k_{mi}[a+h]) - J_v'(k_{mi}[a+h])N_v'(k_{mi}a) = 0. \tag{8}$$

Equation (8) produces an infinite denumerable set of k_{mi} eigenvalues with $i = 1, 2, \cdots$. Arbitrarily set $c_2 = 1$ and determine c_1 from (7a):

$$c_1 = c_{mi} = -N_v'(k_{mi}a)/J_v'(k_{mi}a). \tag{9}$$

The field solution is found from (3) and (4), [7]:

$$E_\rho = -\frac{1}{\rho}A_{mli}\left(\frac{m\pi}{2\theta}\right)R_v(k_{mi}\rho)\cos\left(\frac{m\pi}{2\theta}\phi\right)\cos\left(\frac{l\pi}{2b}z\right) \tag{10a}$$

$$E_\phi = A_{mli}k_{mi}R_v'(k_{mi}\rho)\sin\left(\frac{m\pi}{2\theta}\phi\right)\cos\left(\frac{l\pi}{2b}z\right);\ E_z = 0 \tag{10b}$$

$$H_\rho = \frac{j}{\omega\mu}A_{mli}k_{mi}\left(\frac{l\pi}{2b}\right)R_v(k_{mi}\rho)\cdot\sin\left(\frac{m\pi}{2\theta}\phi\right)\sin\left(\frac{l\pi}{2b}z\right) \tag{10c}$$

$$H_\phi = \frac{j}{\omega\mu\rho}A_{mli}\left(\frac{ml\pi^2}{4\theta b}\right)R_v(k_{mi}\rho)\cdot\cos\left(\frac{m\pi}{2\theta}\phi\right)\sin\left(\frac{l\pi}{2b}z\right) \tag{10d}$$

$$H_z = \frac{-j}{\omega\mu} A_{mli}(k_{mi})^2 R_v(k_{mi}\rho) \sin\left(\frac{m\pi}{2\theta}\phi\right) \cos\left(\frac{l\pi}{2b}z\right). \quad (10e)$$

Cavity resonant frequencies f_r for each mli mode are found from the equation

$$k^2 = p^2 + \left(\frac{l\pi}{2b}\right)^2, \quad (11)$$

and (2c):

$$(f_r)_{mli} = \frac{1}{2\pi\sqrt{\epsilon\mu}} \sqrt{(k_{mi})^2 + \left(\frac{l\pi}{2b}\right)^2}. \quad (12)$$

The TM to z field solution is constructed by choosing $\vec{F} = 0$ and $\vec{A} = \hat{u}_z\psi$. Using (1) and (2) and applying magnetic wall BC's, ψ can be written as

$$\psi_{mli} = B_{mli} R_v(k_{mi}\rho) \cos\left(\frac{m\pi}{2\theta}\phi\right) \sin\left(\frac{l\pi}{2b}z\right). \quad (13)$$

Here B_{mli} is a constant for the mlith mode, $m = 0, 1, \cdots$, and $l = 1, 2, \cdots$, and R_v satisfies (4) with $p = k_{mi}\rho$. Equation (5) still applies. Imposing the electric wall BC's on (5) requires

$$R_v(p)\,|_{\rho=a,\, a+h} = 0, \quad (14)$$

or

$$c_1 J_v(k_{mi}a) + c_2 N_v(k_{mi}a) = 0 \quad (15a)$$

$$c_1 J_v(k_{mi}[a+h]) + c_2 N_v(k_{mi}[a+h]) = 0. \quad (15b)$$

In order that $c_1, c_2 \neq 0$,

$$J_v(k_{mi}a) N_v(k_{mi}[a+h]) - J_v(k_{mi}[a+h]) N_v(k_{mi}a) = 0, \quad (16)$$

which is obtained from (15). Equation (16) produces an infinite denumerable set of k_{mi} eigenvalues with $i = 1, 2, \cdots$. Arbitrarily set $c_2 = 1$ and find c_1 from (15a):

$$c_1 = c_{mi} = -N_v(k_{mi}a)/J_v(k_{mi}a). \quad (17)$$

The field solution is obtained from (4) and (13)

$$E_\rho = \frac{-j}{\omega\epsilon} B_{mli} k_{mi} \left(\frac{l\pi}{2b}\right) R_v'(k_{mi}\rho) \cos\left(\frac{m\pi}{2\theta}\phi\right) \cos\left(\frac{l\pi}{2b}z\right) \quad (18a)$$

$$E_\phi = \frac{j}{\omega\epsilon\rho} B_{mli} \left(\frac{ml\pi^2}{4\theta b}\right) R_v(k_{mi}\rho) \cdot \sin\left(\frac{m\pi}{2\theta}\phi\right) \cos\left(\frac{l\pi}{2b}z\right) \quad (18b)$$

$$E_z = \frac{-j}{\omega\epsilon} B_{mli} k_{mi}^2 R_v(k_{mi}\rho) \cos\left(\frac{m\pi}{2\theta}\phi\right) \sin\left(\frac{l\pi}{2b}z\right) \quad (18c)$$

$$H_\rho = -\frac{1}{\rho} B_{mli} \left(\frac{m\pi}{2\theta}\right) R_v(k_{mi}\rho) \sin\left(\frac{m\pi}{2\theta}\phi\right) \sin\left(\frac{l\pi}{2b}z\right) \quad (18d)$$

$$H_\phi = -B_{mli} k_{mi} R_v'(k_{mi}\rho) \cos\left(\frac{m\pi}{2\theta}\phi\right) \sin\left(\frac{l\pi}{2b}z\right); H_z = 0. \quad (18e)$$

Cavity resonant frequencies are found from (12).

Inspection of the cavity field solutions in (10) for the TE to z modes and (18) for the TM to z modes shows that the complex power density (Poynting vector) $\vec{P} = \vec{E} \times \vec{H}^*$ is purely imaginary. Thus the time average power flow P_{av} out of the walls is zero. This result is expected, however, some comments are in order. For applications where the cavity is used to model a microstrip antenna radiator, the following procedure can be used to obtain radiation. First the cavity field solutions are obtained as it has been done here. Next the field solutions are used as Huygens sources at the open wall (formed by perpendiculars dropped from the antenna patch edges to the conducting surface below) boundaries. These wall fields allow for actual radiation (with the dropping at this stage of the magnetic wall conditions). Finally the radiation problem may be simplified by using the equivalence principle to express the boundary fields alternatively as radiating electric current $\vec{J} = \hat{n} \times \vec{H}_b$ and magnetic current $\vec{M} = \vec{E}_b \times \hat{n}$ sources (b subscript denotes boundary and $\hat{n}$ is normal to wall which points outward from cavity).

Consider the limiting case of the cavity where $h \to 0$. First examine the TM_z modal field solution. Equation (16) can be written as

$$E(p) = J_v(p) N_v(p + \Delta p) - J_v(p + \Delta p) N_v(p) = 0 \quad (19)$$

by letting $p = ak_{mi}$ and $\Delta p = hk_{mi}$. Using Taylor series expansions of the Bessel functions about p and retaining only first order terms in Δp, the left side of (19) can be simplified to read

$$E(p) = [J_v(p) N_v'(p) - J_v'(p) N_v(p)]\, \Delta p \quad (20a)$$

$$= \frac{2}{\pi p}\, \Delta p. \quad (20b)$$

Equation (20b) was obtained from (20a) by identifying the term in brackets as the Wronskian of J_v and N_v. Combining (19) and (20) require that $p \to \infty$. That is, a finite k_{mi} solution to the radial Bessel equation cannot be found for the limiting case of $\Delta p/p \to 0$ or $h/a \to 0$. Thus for physical reasons the TM to z field solution would not be used to obtain the general field solution. For completeness, however, the TM to z field solution will be given for this limiting case. Referring to (17) and (18), and setting $\beta = l\pi/2b$

$$E_\rho = \frac{j}{\omega\epsilon} B_{mli}'\beta \cos(v\phi) \cos(\beta z); \quad E_\phi = E_z = 0 \quad (21a)$$

$$H_\phi = B_{mli}' \cos(v\phi) \sin(\beta z); \quad H_\rho = H_z = 0, \quad (21b)$$

where B_{mli}' is related to B_{mli} by

$$B_{mli}' = -k_{mi} B_{mli} R_v'(k_{mi}a). \quad (22)$$

Next examine the TE_z modal field case. Equation (8) can be expressed as

$$D(p) = J_v'(p) N_v'(p + \Delta p) - J_v'(p + \Delta p) N_v'(p) = 0. \quad (23)$$

Following the same procedure in going from (19) to (20a), the left side of (23) becomes

$$D(p) = [J_v'(p) N_v''(p) - J_v''(p) N_v'(p)]\, \Delta p. \quad (24)$$

Utilizing (4) to eliminate J_v'' and N_v'' in (24) transforms $D(p)$ into

$$D(p) = \frac{v^2 - p^2}{p^2} [J_v'(p) N_v(p) - J_v(p) N_v'(p)]\, \Delta p, \quad (25)$$

which by (20) becomes

$$D(p) = \frac{2}{\pi} \frac{p^2 - v^2}{p^3} \Delta p. \quad (26)$$

From (23) $D(p) = 0$. Imposing this constraint on (26) produces solutions $p = \pm v = \pm m\pi/2$, if $p \neq 0$. Since m is an integer on the domain $(-\infty, \infty)$, $p = v$ is a complete solution statement. For $p = 0$, application of L'Hôpital's rule shows that $D(0) = 0$ and (26) is automatically satisfied. Since $p = 0$ corresponds to $m = 0$, $p = v$ for all m on the integer domain.

The TE to z field solution for the limiting case $\Delta p/p \to 0$ or $h/a \to 0$, referring to (9) and (10), is given by

$$E_\rho = -\frac{1}{a} A_{mi}' \cos(v\phi) \cos(\beta z); \quad E_\phi = E_z = 0 \tag{27a}$$

$$H_\phi = \frac{j}{\omega\mu a} A_{mi}' \beta \cos(v\phi) \sin(\beta z); \quad H_\rho = 0 \tag{27b}$$

$$H_z = \frac{-j}{\omega\mu a^2} A_{mi}' v \sin(v\phi) \cos(\beta z). \tag{27c}$$

Here we have used $k_{mi} = m\pi/2\theta a$, $c_{mi} = c_m$, and

$$A_{mi}' = A_{mli} v R_v(v). \tag{28}$$

Resonant frequencies using (12) are given by

$$(f_r)_{ml} = \frac{1}{2\pi\sqrt{\epsilon\mu}} \sqrt{\left(\frac{m\pi}{2\theta a}\right)^2 + \left(\frac{l\pi}{2b}\right)^2}. \tag{29}$$

The modal $(f_r)_{ml}$ are the same form as found for a planar rectangular cavity with $k_x = n\pi/h = 0$ (i.e., $n = 0$ giving no field variation in the x coordinate direction) for the TE to z modes. This k_x choice produces the same planar rectangular field solution functional form as we found in (27), the correspondence being obvious if the limit $a \to \infty$ is applied and the identifications $a\phi \to y$, $2\theta a \to 2c$, and $\rho \to x$ made ($2c$ is the extent in the rectangular coordinate y direction).

It is interesting to note that the correct field solutions for thin cavities seen in (27) are obtained by solving the electromagnetic problem subject to the constraint that all variation with ρ goes to zero; i.e., $\partial/\partial\rho \to 0$. The procedure of taking $\partial/\partial n \to 0$ where $\hat{n}$ is a unit vector normal to the conformal conducting surface is often applied to microstrip antenna problems and leads to good agreement between theory and experiment [4].

NUMERICAL RESULTS

For illustrative purposes the dimensions of the cylindrical-rectangular cavity will be chosen to be $a = 2$ cm, $b = 1$ cm, $\theta = 24°$. The filling relative dielectric constant is set to $\epsilon_r = 5.0$. From the k_{mi} eigenvalue solutions as determined by (16), the TM_{mli} cylindrical-rectangular frequency eigenvalues f_{rC} are found using (12) and are shown in Table I for $m = 0 - 4$, $i = 1 - 5$, and $l = 1$. The TE_{mli} frequency eigenvalues f_{rC} are found in a similar manner using (8) and (12) and are given in Table II for $m = 1 - 5$, $i = 1 - 5$, and $l = 0$. Both tables provide f_{rC} for $h/a = 0.1, 0.25, 0.50, 0.75$, and 1.00.

The effect of curvature on a patch antenna's f_r can be ascertained by considering the inner radial surface of the cylindrical-rectangular patch antenna to be equal to the patch area of a planar rectangular patch antenna. The radial thickness h is set equal to the planar patch antenna's dielectric substrate thickness. The rectangular dimensions are therefore $x = h$, $y = 2\theta a$, and $z = 2b$. Tables III and V give f_{rR} for the rectangular patch for, respectively, $h/a = 0.1$ and 1.0,

$$f_{rR} = 6.703563 \sqrt{\left(\frac{m}{g}\right)^2 + (5i)^2 + \left(\frac{l}{2}\right)^2} \tag{30}$$

TABLE I
RESONANT FREQUENCIES FOR THE TM_{mli} CYLINDRICAL-RECTANGULAR CAVITY MODES

h/a	i \ m	0	1	2	3	4
	1	33.6812	33.8962	34.5333	35.5697	36.9718
	2	67.1175	67.2257	67.5495	68.0858	68.8296
0.10	3	100.6080	100.6803	100.8969	101.2567	101.7584
	4	134.1122	134.1665	134.3290	134.5996	134.9774
	5	167.6219	167.6653	167.7954	169.0121	168.3149
	1	13.8115	14.2642	15.5424	17.4626	19.8397
	2	27.0187	27.2542	27.9490	29.0704	30.5721
0.25	3	40.3580	40.5162	40.9872	41.7606	42.8202
	4	53.7310	53.8500	54.2054	54.7926	55.6046
	5	67.1177	67.2130	67.4981	67.9706	68.6269
	1	7.4825	8.1474	9.8668	12.1789	14.7789
	2	13.8156	14.1917	15.2733	16.9277	19.0098
0.50	3	20.5138	20.6429	21.4031	22.6161	24.2175
	4	27.0194	27.2159	27.7974	28.7417	30.0166
	5	33.6822	33.8401	34.3096	35.0790	36.1300
	1	5.5724	6.3029	8.0726	10.2890	12.6525
	2	9.5375	10.0002	11.2803	13.1466	15.3735
0.75	3	13.8139	14.1395	15.0777	16.5334	18.3943
	4	18.1835	18.4326	19.1622	20.3261	21.8623
	5	22.5916	22.7928	23.3870	24.3486	25.6408
	1	4.7262	5.4483	7.1178	9.1102	11.1801
	2	7.4856	7.9932	9.3591	11.2583	13.3957
1.00	3	10.5948	10.9612	12.0074	13.5916	15.5506
	4	13.8146	14.1002	14.9289	16.2303	17.9170
	5	17.0867	17.3187	17.9996	19.0894	20.5349

Here m = 0–4, l = 1, i = 1–5. h/a = 0.1, 0.25, 0.50, 0.75, and 1.00. a = 2 cm, b = 1 cm, θ = 24°, and ϵ_r = 5.0.

TABLE II
RESONANT FREQUENCIES FOR THE TE_{mli} CYLINDRICAL-RECTANGULAR CAVITY MODES

h/a	i \ m	1	2	3	4	5
	1	3.8117	7.6230	11.4335	15.2426	19.0499
	2	33.7462	34.3885	35.4334	36.8470	38.5892
0.10	3	67.1499	67.4744	68.0118	68.7571	69.7036
	4	100.6297	100.8464	101.2066	101.7088	102.3508
	5	134.1285	134.2911	134.5618	134.9399	135.4243
	1	3.5617	7.1111	10.6366	14.1282	17.5802
	2	13.9070	15.2470	17.2641	19.7649	22.6058
0.25	3	27.0654	27.7686	28.9038	30.4240	32.2770
	4	40.3889	40.8625	41.6401	42.7055	44.0384
	5	53.7542	54.1107	54.6998	55.5142	56.5444
	1	3.2029	6.2991	9.2463	12.0873	14.8769
	2	7.5291	9.5525	12.2791	15.3210	18.4424
0.50	3	13.8246	14.9569	16.6934	18.8978	21.4561
	4	20.3896	21.1657	22.4043	24.0413	26.0124
	5	27.0236	27.6119	28.5674	29.8576	31.4452
	1	2.8864	5.5190	7.9754	10.3760	12.7559
	2	5.5236	7.8925	10.6914	13.4310	16.0361
0.75	3	9.4744	10.8904	13.0029	15.6052	18.4076
	4	13.7656	14.7470	16.2770	18.2622	20.6383
	5	18.1452	18.8938	20.0890	21.6723	23.5902
	1	2.6013	4.8545	6.9824	9.0795	11.1614
	2	4.5719	7.0171	9.4999	11.8068	14.0445
1.00	3	7.3312	8.9682	11.3300	13.8735	16.2729
	4	10.4740	11.6081	13.3685	15.6580	18.2029
	5	13.7212	14.5878	15.9578	17.7725	20.0038

Here m = 1–5, l = 0, i = 1–5. Same cavity dimensions as in Table I.

TABLE III
RESONANT FREQUENCIES FOR THE TM_{mli} RECTANGULAR CAVITY MODES FOR $l = 1$ AND $h/a = 0.1$ WITH $g = 1.675516$ IN (30)

i \ m	0	1	2	3	4
1	33.68499	33.92176	34.62235	35.75951	37.29334
2	67.11938	67.23851	67.59467	68.18413	69.00091
3	100.60930	100.68882	100.92700	101.32273	101.87416
4	134.11316	134.17282	134.35165	134.64919	135.06463
5	167.62260	167.67034	167.81348	168.04877	168.38482

TABLE IV
RESONANT FREQUENCIES FOR THE TM_{mli} RECTANGULAR CAVITY MODES FOR $l = 1$ AND $h/a = 0.1$ WITH $g = 1.759292$ IN (30)

i \ m	0	1	2	3	4
1	33.68499	33.89981	34.53628	35.57175	36.97272
2	67.19375	67.22745	67.55062	68.08584	68.82815
3	100.60930	100.68143	100.89750	101.25661	101.75723
4	134.11316	134.16728	134.32950	134.59944	134.97645
5	167.62260	167.66590	167.79574	168.01192	168.31411

TABLE V
RESONANT FREQUENCIES FOR THE TM_{mli} RECTANGULAR CAVITY MODES FOR $l = 1$ AND $h/a = 1.0$ WITH $g = 1.675516$ IN (30)

i \ m	0	1	2	3	4
1	4.740135	6.202906	9.300404	12.904778	16.690818
2	7.494811	8.495844	10.963614	14.150499	17.671636
3	10.599264	11.329234	13.280550	16.012770	19.195284
4	13.819749	14.387238	15.969161	18.304368	21.144739
5	17.090799	17.552851	18.871249	20.884440	23.413884

with $g = 1.675516$. Equation (30) gives f_{rR} in GHz. For nontrivial TM_z rectangular patch field solutions $i = 1, 2, \cdots, m = 0, 1, \cdots$, and $l = 1, 2, \cdots$. These eigennumbers correspond exactly to those in Table I. Comparison of the f_{rC} and f_{rR} eigenvalues in Table I and Table III for $h/a = 0.1$ shows the largest difference being 0.87 percent. As i increases the difference is reduced, but as m increases, the difference is increased. This same f_r behavior with varying i and m occurs for $h/a = 1.0$ in Tables I and V with the largest difference being 4.4 percent. For the TE_z rectangular patch fields, having nontrivial solutions at $i = 0, 1, \cdots, m = 1, 2, \cdots, l = 0, 1, \cdots$, the difference is about an order of magnitude larger. Tables II and VII for $h/a = 0.1$ demonstrate that the largest f_r difference is 5.2 percent, and Tables II and IX for $h/a = 1.0$ that this value is enlarged to 79.2 percent.

The TE_{m10} cylindrical-rectangular eigenvalues correspond to the two-dimensional resonating modes of the planar rectangular patch antenna which have no field variation normal to the patch surface. These modes are often utilized in planar microstrip antenna analysis, and have f_{rR} and f_{rC} differing by less than 5 percent for $h/a = 0.1$.

Tables IV, VI, VIII, and X provide f_{rR} calculated using (30) with $g = 1.759292$ ($h/a = 0.1$) or 2.513274 ($h/a = 1.0$). Using these g values means that an equivalent rectangular cavity (to the cylindrical-rectangular cavity) has been found because an average radius $r = a + h/2$ has been chosen for one side of the cylindrical-rectangular cavity. One might expect f_{rR} to be extremely close to f_{rC}. Agreement is within 0.011 percent for $h/a = 0.1$ and 4.4 percent for $h/a = 1.0$ for the TM_z modes. For the TE_z modes, agreement is within, respectively, 0.035 percent and 19.5 percent for $h/a = 0.1$ and 1.0.

TABLE VI
RESONANT FREQUENCIES FOR THE TM_{mli} RECTANGULAR CAVITY MODES FOR $l = 1$ AND $h/a = 1.0$ WITH $g = 2.513274$ IN (30)

i \ m	0	1	2	3	4
1	4.740135	5.439042	7.136249	9.300404	11.674654
2	7.494811	7.955281	9.758303	10.963614	13.038438
3	10.599264	10.929716	11.865983	13.280550	15.039051
4	13.819749	14.074792	14.813596	15.969161	17.458927
5	17.090799	17.297679	18.681803	18.871249	20.147558

TABLE VII
RESONANT FREQUENCIES FOR THE TE_{mli} RECTANGULAR CAVITY MODES FOR $l = 1$ AND $h/a = 0.1$ WITH $g = 1.675516$ IN (30)

i \ m	1	2	3	4	5
0	4.00089	8.00179	12.00269	16.00358	20.00447
1	33.75576	34.45973	35.60208	37.14245	39.03361
2	67.15492	67.51151	68.10170	68.91945	69.95681
3	100.63301	100.87133	101.26727	101.81901	102.52402
4	134.13094	134.30984	134.60746	135.02303	135.55546

TABLE VIII
RESONANT FREQUENCIES FOR THE TE_{mli} RECTANGULAR CAVITY MODES FOR $l = 1$ AND $h/a = 0.1$ WITH $g = 1.759292$ IN (30)

i \ m	1	2	3	4	5
0	3.81038	7.62075	11.43113	15.24150	19.05188
1	33.73371	34.37324	35.41348	36.82048	38.55409
2	67.14384	67.46741	68.00329	68.74649	69.69039
3	100.62562	100.84182	101.20112	101.70201	102.34242
4	134.12540	134.28768	134.55770	134.93483	135.41816

TABLE IX
RESONANT FREQUENCIES FOR THE TE_{mli} RECTANGULAR CAVITY MODES FOR $l = 1$ AND $h/a = 1.0$ WITH $g = 1.675516$ IN (30)

i \ m	1	2	3	4	5
0	4.008949	8.0017895	12.002685	16.003579	20.004474
1	5.219349	8.6754289	12.461896	16.350809	20.283328
2	7.806723	10.438697	13.747806	17.350858	21.097789
3	10.822066	12.850626	15.658045	18.900383	22.389482
4	13.991361	15.613445	17.994873	20.877393	24.081735

TABLE X
RESONANT FREQUENCIES FOR THE TE_{mli} RECTANGULAR CAVITY MODES FOR $l = 1$ AND $h/a = 1.0$ WITH $g = 2.513274$ IN (30)

i \ m	1	2	3	4	5
0	2.667263	5.334526	8.001789	10.669052	13.336315
1	4.283542	6.300128	8.675429	11.183162	13.751063
2	7.214711	8.567084	12.026731	12.600255	14.926321
3	10.403088	11.382755	12.850626	14.660785	16.702313
4	13.669869	14.429421	15.613445	17.134167	18.910535

CONCLUSION

The field distribution within a cylindrical-rectangular microstrip antenna has been determined using a cavity modal model for the TE_z and TM_z modes. Resonant frequency eigenvalue equations for these modes were used to calculate the eigenfrequencies $(f_r)_{mli}$ for some of the lowest order modes.

Comparison of $(f_r)_{mli}$ for the cylindrical-rectangular case f_{rC}, and $(f_r)_{mli}$ for a planar rectangular microstrip antenna f_{rR}, allows an assessment of the effect curvature has on resonant frequency. Numerical results show that curvature changes f_r by less than about 5 percent for a substrate dielectric thickness equal to one tenth of the radius of curvature. The exact effect of curvature on f_r will be dependent on the particular choice of antenna parameters, but the results found in this communication should be a useful guide when designing conformal microstrip antennas.

An equivalent rectangular microstrip planar antenna to the cylindrical-rectangular microstrip antenna had been defined. Agreement between f_{rR} and f_{rC} is better than 0.035 percent.

REFERENCES

[1] K. R. Carver and J. W. Mink, "Microstrip antenna technology," *IEEE Trans. Antennas Propagat.*, vol. AP-29, no. 1, pp. 2–24, Jan. 1981.

[2] Y. T. Lo, D. Solomon, and W. F. Richards, "Theory and experiment on microstrip antennas," *IEEE Trans. Antennas Propagat.*, vol. AP-27, no. 2, pp. 137–145, Mar. 1979.

[3] R. F. Harrington, *Time-Harmonic Electromagnetic Fields*. New York: McGraw-Hill, 1961, p. 480.

[4] M. Abramowitz and I. A. Stegun, *Handbook of Mathematical Functions with Formulas, Graphs, and Mathematical Tables*. Nat. Bur. Stand. Appl. Math. Ser., 1972, p. 1046.

[5] H. Sagan, *Boundary and Eigenvalue Problems in Mathematical Physics*. New York: Wiley, 1961, p. 381.

[6] R. V. Churchill, *Fourier Series and Boundary Value Problems*. New York: McGraw-Hill, 1941, p. 206.

[7] C. M. Krowne, "Cylindrical-rectangular microstrip antenna radiation efficiency based on cavity Q factor," *IEEE Antennas Propagat. Int. Symp. Soc. Dig.*, June 1981, pp. 11–14. (Note that in (7a) of this paper, k_{0i} in the numerator needs a factor of 2. Same factor is needed for R in (7b).)

Combined E- and H-Plane Phase Centers of Antenna Feeds

PER-SIMON KILDAL, MEMBER, IEEE

Abstract—**The feed efficiency, a first approximation to the aperture efficiency of a paraboloid or a conventional Cassegrain antenna, is used to define uniquely a combined E- and H-plane phase center of the feed pattern. A formula for numerical calculation of the combined phase center is presented, as well as theoretical results of the feed position tolerances and the efficiency loss due to differences in the principal plane phase patterns.**

I. INTRODUCTION

For designing a reflector antenna system, it is important to know the feed phase center since it determines the location of the feed relative to the focal point of the reflector. Too large a deviation between the two points causes severe defocusing of the secondary radiation pattern. The phase center of an antenna is ideally the center of a portion of a sphere on which the radiation field of the antenna has a constant phase [1], [2]. However, in many cases the phase patterns are oscillatory, so that an ideal phase center does not exist. A more practical definition of the phase center has been given by Rusch and Potter [3, p. 147], as the center of the "best" nearly constant-phase spheres in a least squares sense. Although the definition given by Rusch and Potter is general enough to obtain a combined E- and H-plane phase center within a given solid angle, practical formulas were given only for numerical calculation of a phase center in a single principal plane. This communication presents a practical formula for calculation of a combined E- and H-plane phase center, and is therefore an important supplement to Rusch and Potter's work.

The results in this communication are obtained by a slightly different general definition. The feed for a paraboloid or a conventional Cassegrain reflector system is located in such a way that the phase reference point of the feed pattern coincides with the focal point of the reflector system. The phase center is then defined as the phase reference point which maximizes the feed efficiency, the latter being the first-order approximation to the aperture efficiency of the paraboloid or the Cassegrain system. This definition is equivalent to that of Rusch and Potter [3] for a proper choice of weighting functions in the least-squares calculation. The resulting calculation formula for the overall phase center is therefore also very similar to the formula for the principal plane phase center. The tolerances on the phase-center position (corresponding to the axial tolerances on the position of the feed in the reflector antenna) and the efficiency losses due to differences in the principal plane phase patterns are also discussed.

II. MATHEMATICAL FORMULATION

We assume a far-field feed pattern, which is linearly polarized and determined by its E-plane pattern $A(\psi)$ and H-plane pattern $C(\psi)$, according to

$$\vec{E}(\psi, \xi, \rho) = [A(\psi) \sin \xi \, \vec{a}_\psi + C(\psi) \cos \xi \, \vec{a}_\xi] \, \frac{1}{\rho} \, e^{-jk\rho} \tag{1}$$

where $\vec{a}_\psi$ and $\vec{a}_\xi$ are unit vectors in the direction of increasing polar angle ψ and azimuth angle ξ, respectively. Equation (1) assumes that $A(\psi)$ and $C(\psi)$ are given with respect to the same phase reference point O, positioned at $z = 0$ and that ρ is the distance from O to the far-field point (Fig. 1). $A(\psi)$ and $C(\psi)$ can be transformed to a new phase reference point P positioned at $z = \delta$, by the relations

$$A_\delta(\psi) = A(\psi) e^{-jk\delta \cos \psi}, \qquad C_\delta(\psi) = C(\psi) e^{-jk\delta \cos \psi}. \tag{2}$$

Then the far field is given by (1) if $A_\delta(\psi)$ and $C_\delta(\psi)$ replace $A(\psi)$ and $C(\psi)$, respectively, and if ρ now is the distance from P to the far-field point.

We consider the feed to be located in the primary focus of a paraboloidal antenna or in the secondary focus of a conventional Cassegrain antenna (hyperboloid–paraboloid configuration) in such a way that the point P coincides with the proper focal point. Then the first approximation to the aperture efficiency of the reflector antenna, excluding the effects of blockage and subreflector diffraction in the Cassegrain, is

$$\eta_f = \cot^2 \left(\frac{\psi_0}{2} \right) \frac{\left| \int_0^{\psi_0} [A_\delta(\psi) + C_\delta(\psi)] \tan \frac{\psi}{2} \, d\psi \right|^2}{\int_0^{\pi} [\,|A_\delta(\psi)|^2 + |C_\delta(\psi)|^2] \sin \psi \, d\psi} \tag{3}$$

Manuscript received March 29, 1982; revised June 29, 1982. This work was supported by the Norwegian Council for Scientific and Industrial Research.

The author is with Electronics Research Laboratory, The Norwegian Institute of Technology, O. S. Bragstads Plass 6, N-7034, Trondheim-NTH, Norway.

0018-926X/83/0100-0199$1.00 © 1983 IEEE